Study of PEGylated Lipid Layers as a Model for PEGylated Liposome Surfaces: Molecular Dynamics Simulation and Langmuir Monolayer Studies

ARTICLE *in* LANGMUIR · JUNE 2011

Impact Factor: 4.46 · DOI: 10.1021/la200003n · Source: PubMed

10 AUTHORS, INCLUDING:

Marta Pasenkiewicz-Gierula
Jagiellonian University
93 PUBLICATIONS **2,782** CITATIONS
SEE PROFILE

Tomasz Róg
Tampere University of Technology
136 PUBLICATIONS **3,241** CITATIONS
SEE PROFILE

Mikko Karttunen
Technische Universiteit Eindhoven
229 PUBLICATIONS **6,287** CITATIONS
SEE PROFILE

Alex Bunker
University of Helsinki
58 PUBLICATIONS **718** CITATIONS
SEE PROFILE

Langmuir

ARTICLE

pubs.acs.org/Langmuir

Study of PEGylated Lipid Layers as a Model for PEGylated Liposome Surfaces: Molecular Dynamics Simulation and Langmuir Monolayer Studies

Michał Stepniewski,[†,§] Marta Pasenkiewicz-Gierula,[§] Tomasz Róg,[∥,#] Reinis Danne,[∥] Adam Orlowski,[∥,§] Mikko Karttunen,[○] Arto Urtti,[†] Marjo Yliperttula,[‡] Elina Vuorimaa,[⊥] and Alex Bunker*[,†,▽]

[†]Centre for Drug Research and [‡]Division of Biopharmacy, Faculty of Pharmacy, University of Helsinki, Helsinki, Finland

[§]Department of Computational Biophysics and Bioinformatics, Jagiellonian University, Krakow, Poland

[∥]Department of Physics and [⊥]Department of Chemistry and Bioengineering, Tampere University of Technology, Tampere, Finland

[#]Department of Applied Physics and [▽]Department of Chemistry, Aalto University, Espoo, Finland

[○]Department of Applied Mathematics, The University of Western Ontario, London, Ontario, Canada

Supporting Information

ABSTRACT: We have combined Langmuir monolayer film experiments and all-atom molecular dynamics (MD) simulation of a bilayer to study the surface structure of a PEGylated liposome and its interaction with the ionic environment present under physiological conditions. Lipids that form both gel and liquid-crystalline membranes have been used in our study. By varying the salt concentration in the Langmuir film experiment and including salt at the physiological level in the simulation, we have studied the effect of salt ions present in the blood plasma on the structure of the poly(ethylene glycol) (PEG) layer. We have also studied the interaction between the PEG layer and the lipid bilayer in both the liquid-crystalline and gel states. The MD simulation shows two clear results: (a) The Na^+ ions form close interactions with the PEG oxygens, with the PEG chains forming loops around them and (b) PEG penetrates the lipid core of the membrane for the case of a liquid-crystalline membrane but is excluded from the tighter structure of the gel membrane. The Langmuir monolayer results indicate that the salt concentration affects the PEGylated lipid system, and these results can be interpreted in a fashion that is in agreement with the results of our MD simulation. We conclude that the currently accepted picture of the PEG surface layer acting as a generic neutral hydrophilic polymer entirely outside the membrane, with its effect explained through steric interactions, is not sufficient. The phenomena we have observed may affect both the interaction between the liposome and bloodstream proteins and the liquid-crystalline−gel transition and is thus relevant to nanotechnological drug delivery device design.

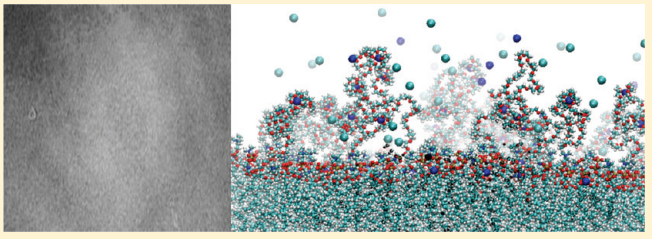

INTRODUCTION

Nanoscale devices capable of carrying, protecting, and in some cases directing drug molecules to their target are a promising technology for the improvement of drug delivery.[1] Liposomes are vesicles of lipid bilayers that have been used for drug delivery since the 1970s.[2] The phospholipids that make up the liposome are unfortunately vulnerable to attack from the immune system. The liposomes first adhere proteins in the blood plasma (i.e., opsonization[3]) and thereafter are recognized and removed from blood circulation by macrophages in the liver and spleen.[4,5] As a result, liposomes have a short half-life in the bloodstream (∼1 h), which blocks their applicability in drug targeting of tumors or other targets.

The circulation time of liposomes in the bloodstream can be prolonged by an order of magnitude using lipids with hydrophilic polymers attached to their headgroups.[6,7] The polymers form a steric and entropic barrier protecting the liposome. Although several different polymer coatings have been explored, poly(ethylene glycol) (PEG) has shown particular promise. When PEG is used, the resulting liposomes are commonly referred to as being PEGylated.

PEGylated liposomes have found uses as pharmaceutical carriers for the delivery of a variety of therapies.[8] The most notable clinical application is cancer therapy,[9−11] with doxorubicin encapsulated in a PEGylated liposome.[12,13] Other applications of liposomes and nanoparticles include combating infectious agents,[14] gene therapy,[15] and medical imaging.[16] As in liposomes, PEG has been broadly applied as a half-life-increasing coating for nanoparticles[17] and as a conjugate for proteins[18] and other drugs.[19] The structure, metabolism, and clinical efficacy of

Received: January 1, 2011
Revised: May 3, 2011
Published: May 23, 2011

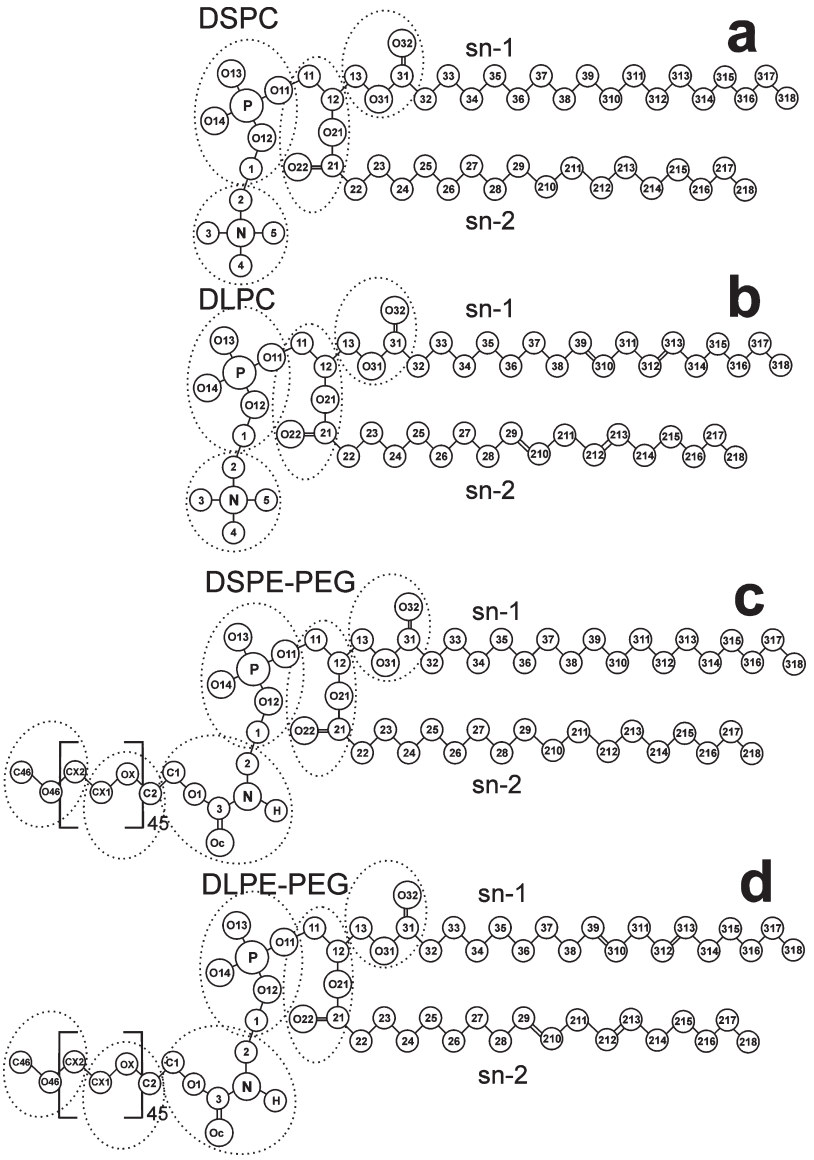

Figure 1. Chemical structures of the (a) DSPC, (b) DLPC, (c) DSPE-PEG, and (d) DLPE-PEG molecules.

PEGylated liposomes have been studied extensively.[4,20−23] Usually in intravenously applied pharmaceutical liposomes the lipid membrane is in the gel phase. Liposomes that can be thermally driven to undergo a transition from the gel to the liquid-crystalline state in order to achieve triggered release have recently been investigated.[24]

Although PEGylation greatly increases the circulation time of liposomes from an hour to 1 to 2 days,[4] PEGylated liposomes are still opsonized and a major fraction of them are distributed to the liver and spleen. In comparison, red blood cells, blood platelets, and some antibodies have a blood plasma circulation time in the range of months. There is still a great deal of room for improvement in the design of PEGylated liposomes.

Lipid bilayers with grafted polymers, such as a PEGylated membrane, have been studied theoretically[25] and computationally.[26,27] In the resulting model, the PEG surface forms a layer of neutral generic hydrophilic polymer entirely outside the membrane. According to this picture, the static structure of the PEG layer can be modeled as a grafted polymer brush, which is a system that is well understood theoretically[28−30] and through computational[31−34] modeling. This assumption has also been made in the interpretation of experimental work[35−38] as discussed comprehensively in the review article of Needham and Kim.[39] In spite of the success of this conceptual picture, for example, in modeling bilayer−bilayer interactions of membranes in the gel state,[36] there are several factors that have been overlooked.

Until now, the effects of the microscopic interactions between the salt ions in the blood plasma and the PEGylated bilayer have not been considered systematically. Reports by Cohen et al.[40] Janzen et al.[41] indicate that in the presence of salts the PEG layer of a PEGylated liposome may become thinner, but not all of their results consistently support this picture. The interaction of the PEG layer with the salt ions is not a surprise because PEG is known to be capable of dissolving salts[42] (acting as a polymer electrolyte[42]) and is used in lithium ion batteries in this role. A computational[42,43] study of PEG has revealed that cations can bind to multiple PEG oxygens, forming loop structures around cations. Subsequently, a significant number of further

dx.doi.org/10.1021/la200003n |*Langmuir* 2011, 27, 7788–7798

computational,[44−48] theoretical,[49,50] and experimental[48,51−59] studies have demonstrated that cations bind to the PEG oxygens to form both loop structures within individual PEG polymers and effective cross-links between PEG polymers, but the role of these interactions in the PEGylated lipid bilayers has not been investigated.

PEGylated liposomes are considered to have a hydrophilic PEG sheath around them, but actually PEG is not a generic hydrophilic polymer. Although PEG is perfectly soluble in water, it has been found to be soluble in a wide variety of both polar and nonpolar solvents.[60] As such, the assumption that PEG is found entirely outside the membrane, common to both assumptions of the theoretical models,[61] and the interpretations of the experimental results[35−39] may not necessarily be valid. In addition, Nowakowska et al. have obtained experimental results[62] that suggest that PEG penetrates the interior of lipid membranes.

In this study, we carried out experimental and molecular dynamics simulation studies of PEGylated bilayers of gel-state and liquid-crystalline-state lipids in the presence of salt ions. This study provides a corrected and more accurate view of the interactions of salts, PEG, and lipids on the liposome surface. Although we have not directly studied entire liposomes in either the experimental or computational components of the study, both our experimental and computational systems are designed to model the surface structure of liposomes and as such act as models of the liposome surface.

METHODS

Choice of System to Study. MD simulations of membrane bilayers and Langmuir film experiments on monolayers, both involving mixed systems of PEG-phosphatidylethanolamine/phosphatidylcholine (PE-PEG_{2000}/PC) in an approximately 1:9 molar ratio, were combined to study the surface structure of PEGylated liposomes.

In both our simulation and experiment, we studied systems with lipid tails known[63] to display gel and liquid-crystalline states, respectively, in the pure form under physiological conditions (310 K and atmospheric pressure). The two systems chosen for the computational study were roughly designed to replicate the commonly used PEG inclusion ratio in PEGylated liposomes,[7,20] to be based on lipid systems where the computational model of the system is well known to be accurate, and to display gel and liquid-crystalline states, as we have seen in our previous study of pure DSPC and DLPC membranes.[64]

We chose 1,2-distearoyl-*sn*-glycero-3-phosphatidylcholine (DSPC) as the unmodified lipid for the gel system. For the simulation of the liquid-crystalline membrane, we used 1,2-dilinoleoyl-*sn*-glycero-3-phosphatidylcholine (DLPC). Figure 1 shows the chemical structures of the four molecules from which the membranes are composed in our simulations. Because DLPE-PEG_{2000}, 1,2-dilinoleoyl-*sn*-glycero-3-phosphatidylethanolamine-*N*-[methoxy(polyethyleneglycol)-2000] is not commercially available, we instead chose a 1,2-dioleoyl-*sn*-glycero-3-phosphatidylcholine (DOPC)-based system for the Langmuir film experiments. DOPC differs from DLPC in possessing one rather than two double bonds in each of the hydrocarbon tails. The behavior of DOPC at the air−water interface is very similar to that of DLPC, and thus this substitution is acceptable.[65,66]

Although it is known that the inclusion of PEGylated lipid will lower the phase-transition temperature,[37,38] it has been determined experimentally that in the range of the PEG concentration that we have simulated, the DSPC/DSPE-PEG_{2000} system is still in the gel phase.[35] Our previous studies show that MD simulations that make use of our selected methodology correctly reproduce the bilayer phase under physiological conditions for these particular lipids.[64] The length of PEG chains on the lipids in the simulations and experiments was 45 monomer units (a molecule weight of about 2000).

Table 1. Number of Molecules in the Two Systems Studied (Gel and Liquid-Crystalline Bilayer)

system	gel	liquid crystal
DSPC	256	
DSPE-PEG	32	
DLPC		464
DLPE-PEG		48
water	20 386	61 172
Na^+	50	148
Cl^-	18	100

Monolayers containing mixtures of PEGylated and unmodified phospholipids have been used as close approximations of liposome membranes.[67,68] Monolayers are the simplest membrane-mimetic surfaces. The power of a monolayer, particularly when compared to the bilayer and vesicle models, lies in its controllability. Continuous observation of monolayer morphology upon compression offers a unique opportunity to monitor the properties of the film.

Experiment. In these studies DSPC, DSPE-PEG_{2000}, DOPE-PEG_{2000} (Avanti Polar Lipids), and DOPC (Sigma-Aldrich) were used without further purification. The lipids were dissolved in chloroform to a concentration of 0.5 mM. The full isotherms were measured with a KSV OPTREL BAM300 (BAM) mounted on a KSV minitrough Langmuir balance (KSV Instruments) equipped with a double barrier system. Sodium chloride solutions (10, 140, and 500 mM) in Milli-Q water with a resistivity of greater than 18.0 MΩ cm were used as subphases. The temperature of the subphase was 19.5 ± 0.5 °C, and the compression speed was 3 mm min^{-1} (i.e., 2.25 cm^2 min^{-1}). Although the experiment and simulation that we have combined in our study were carried out at separate temperatures, this should not be a reason for concern. Measurements of the pressure−area isotherms for these systems in the range 10 to 37 °C can be found in the literature,[69,70] and only minor changes in the isotherms have been observed in this temperature range. Because no phase boundary is approached, there will be no change in the qualitative behavior of the systems and all quantities can be reliably extrapolated. The solutions were spread on the subphases drop by drop, and the system was allowed to stabilize for 2 min before compression was started. The initial areas per lipid for the four systems were as follows: 1.4 nm^2 for DSPC/DSPE-PEG_{2000}, 3.0 nm^2 for DOPC/DOPE-PEG_{2000}, 0.78 nm^2 for pure DSPC, and 2.1 nm^2 for pure DOPC.

The instrument was equipped with a 10 mW HeNe laser (633 nm) linearly polarized in the plane of incidence by a Glann-Thompson polarizer. The reflection from the interface passed through a second Glann-Thompson polarizer and was received by a CCD camera. The microscope was adjusted so that reflection from the bare air−water interface was minimal. As a result, it was sensitive to local changes in the optical properties of the interface. The spatial resolution of the system was approximately 2 μm. The image-processing procedure included a geometrical correction of the image as well as a filtering operation to reduce noise. Furthermore, the brightness of each image was scaled to improve contrast.

Simulation. To simulate physiological conditions, simulations were carried out at a constant pressure of 1 bar, physiological temperature (310 K), and physiological salt concentration (140 mM NaCl solution). The number of Na^+ and Cl^- ions present in the system was set to preserve both charge neutrality and the molarity of the NaCl solution. Each PEGylated lipid had a total charge of −1, located at the phosphate group. Because both the experiment and simulation were performed at neutral pH, protonation could be assumed not to occur, thus a Na^+ counterion needed to be added for every PEGylated lipid present.

Table 1 shows the number of molecules and ions of each type in both systems. The Jorgensen potential[71] was used for the ionic potentials; the choice of this potential has been found to be important.[72]

To parametrize DSPC, DLPC, DSPE-PEG$_{2000}$, and DLPE-PEG$_{2000}$ molecules and the ions present in the solution, we used the all-atom OPLS force field,[71] and the implementation of this is described in our previous studies.[73−75] Partial charges on the PC headgroups were taken from Takaoka et al.[76] because they were derived in compliance with the OPLS methodology. In all other cases, the partial charges were taken from the OPLS set. Charge groups were chosen to be small to avoid spurious artifacts that may arise if the charge groups are spatially too large.[77] The details of how the charge groups have been defined can be seen in our previous work.[75] The charge groups for a PEG fragment and the linker that connects it to the phospholipid are also shown in Figure 1. The validation of our all-atom model for the PEG polymer is included in the Supporting Information. For water, we employed the TIP3P model that is compatible with the OPLS-AA parametrization.[78]

The initial structures of the DSPC and DLPC bilayer were taken from our previous studies.[64] To construct the PEGylated bilayer, PEG fragments were added gradually to the bilayer one PEG monomer at a time. Each time a new PEG monomer was added, the energy of the system was minimized using the steepest-descent algorithm, after which a short 10 ps MD simulation was run. With increasing PEG length, the layer of water was also gradually increased until the system size in the direction perpendicular to the membrane was approximately 20 nm. Once the PEG chains had reached full length, we performed a 20 ns MD simulation during which the PEG chains relaxed back down toward the membrane. This allowed us to remove the excess water, reducing the dimension of the system perpendicular to the membrane to 15 nm. At this point, we increased the size of the membrane being analyzed by 4-fold through replicating the system over periodic images. The simulations were performed by using the GROMACS 4.0 software package.[79] For both systems, the MD simulations were carried out over 200 ns, of which 100 ns was considered to be the equilibration time, determined from the time needed for ions to adsorb to the polymer layer and the membrane interface. Other parameters that we monitored, related to the structural properties of the lipid bilayer and polymer brush, equilibrated in a shorter time. Verification that our system is not affected by finite size effects was performed, and this is discussed in further detail in the Supporting Information.

Periodic boundary conditions with the usual minimum image convention were used in all three directions. The linear constraint solver (LINCS) algorithm[80] was used to preserve covalent bond lengths. The time step was set to 2 fs. The temperature and pressure were controlled by using the Nosé−Hoover[81,82] and Parrinello−Rahman methods,[83] respectively. The temperatures of the solute and solvent were controlled independently. For pressure, we used semi-isotropic control. The Lennard-Jones interactions were cut off at 1.0 nm, and for the electrostatic interactions, we employed the particle mesh Ewald method.[84,85]

COMPUTATIONAL RESULTS

Effect of PEGylation on Bilayer Properties. We first calculated the time development of the area per lipid molecule in both bilayers, as shown in Figure 2. The area per lipid for the DSPC/DSPE-PEG$_{2000}$ system slowly decreased over the whole simulation time starting from approximately 0.480 ± 0.003 nm^2 and equilibrated to approximately 0.460 ± 0.003 nm^2, a typical value for the gel phase of phospholipid membranes. As expected, the areas in the liquid-crystalline membrane system, DLPC/DLPE-PEG$_{2000}$, reached an equilibrium value far more quickly (40 ns) and exhibited considerably larger fluctuations. The value reached equilibrium at approximately 0.700 ± 0.005 nm^2, a typical value

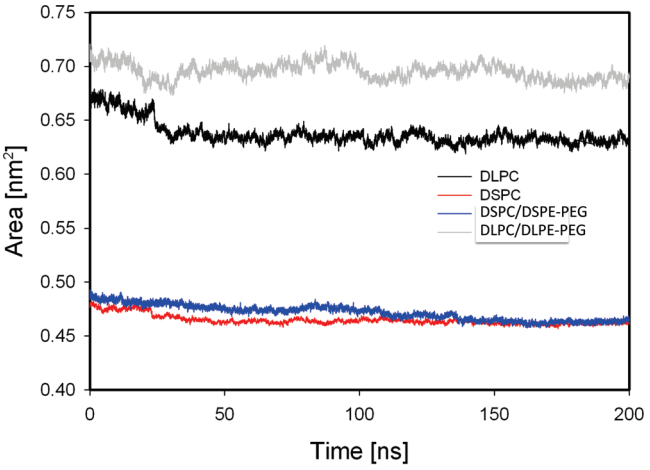

Figure 2. Time development of the surface area for both the gel (DSPC/DSPE-PEG) and liquid-crystalline (DLPC/DLPE-PEG) systems. Data from our previous study of the pure DSPC and DLPC systems is included to show the effect of PEGylation on both the gel and liquid-crystalline systems.

for the liquid-crystalline phase of a phospholipid membrane, for example, the experimentally obtained value of 0.67 nm^2 for DOPC[86] and the value of our computational result for pure DSPC of 0.633 ± 0.002 nm^2.[64] We did not set out to make any quantitative comparison between this value and our experimental results because the pressures between monolayers and bilayers do not match. The monolayer data that is relevant to bilayers must be taken at a higher surface pressure, and the data here is consistent with this fact. Although a direct quantitative comparison from monolayer and bilayer data is not possible, previous examples in the literature exist where insight has been gained from a combination of bilayer and monolayer data.[87,88]

In Figure 2, we also include the surface area results from our previous study of pure DSPC and DLPC membranes.[64] Our results show that the presence of PEG increases the area per lipid molecule in the liquid-crystalline but not the gel phase. It can also be seen that there is still a small amount of drift in the area per lipid result occurring during the measurement phase (100 to 200 ns) of our simulation. Although this means that our system has not completely reached equilibrium, the effect will be negligible and certainly will not qualitatively affect our conclusions. We also calculated the deuterium order parameter along the chains for both systems. (A plot of the data is included in the Supporting Information.) As expected from the trends in the area per lipid data, the presence of PEG does not affect the degree of order of the lipid chains in the gel system and decreases the degree of order in the liquid-crystalline system. To illustrate the membrane structures, snapshots of both systems at the end of the simulation run (alongside the pure system results from our previous publication[64]) are shown in Figure 3. These snapshots illustrate the liquid-crystalline state of the DLPC/DLPE-PEG$_{2000}$ bilayer and the gel phase of the DSPC/DSPE-PEG$_{2000}$ bilayer. We also measured the effect of PEGylation on the water ordering in the vicinity of the membrane, and these results are discussed in the Supporting Information. Animation of the two systems is included as files DSPC_trajectory.mpg and DLPC_trajectory.mpg, and rotating still images are included as files DSPC_still.mpg and DLPC_still.mpg in the Supporting Information.

PEG−Lipid Interaction and Structuring of the PEG Layer. The mass density profile of PEG and the lipid chains along the membrane normal is shown in Figure 4. For the case of DSPC/DSPE-PEG_{2000} (the gel phase), PEG has a single density peak almost entirely outside the region of the lipid tails whereas for the DLPC/DLPE-PEG_{2000} bilayer (the liquid-crystalline phase) we observe that in addition to the main peak outside the membrane there is a second peak among the lipid tails. This indicates that some PEG chains are able to enter the membrane in the more loosely packed structure of the liquid-crystalline membrane but PEGs are completely excluded from the more tightly packed structure of the gel membrane.

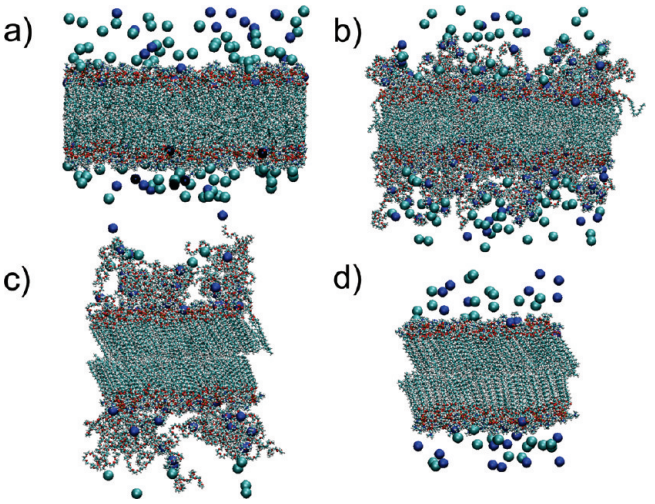

Figure 3. Snapshots of our two PEGylated configurations alongside pure systems (a) DLPC, (b) DLPC/DLPE-PEG, (c) DSPC/DSPE-PEG, and (d) DSPC. Note the distribution of Cl^- (turquoise) and Na^+ (blue) in the four systems (details discussed in the text).

Direct observation of the trajectory was used to determine that, for the DLPC/DLPE-PEG_{2000} bilayer (the liquid-crystalline phase), some entire PEG molecules could be entirely inside the lipid layer. Cases of PEG chains looping into the lipid layer to re-emerge into the water were also apparent (animation in the Supporting Information). From the mass density profile along the membrane normal of the phosphate atoms of the DLPE-PEG_{2000} molecules and of the phosphate atoms of the DLPC molecules, it was determined that the phosphate atoms of the DLPE-PEG_{2000} molecules were at the same height as the phosphate of the DLPC molecules. Thus, as expected, the PEG chains enter the membrane interior without any perturbation of the position of the phosphate headgroup.

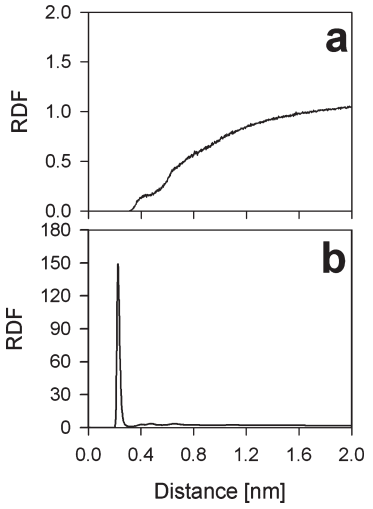

Figure 5. Radial distribution function of (a) Cl^- ions relative to PEG carbon atoms and (b) Na^+ ions relative to PEG oxygen atoms.

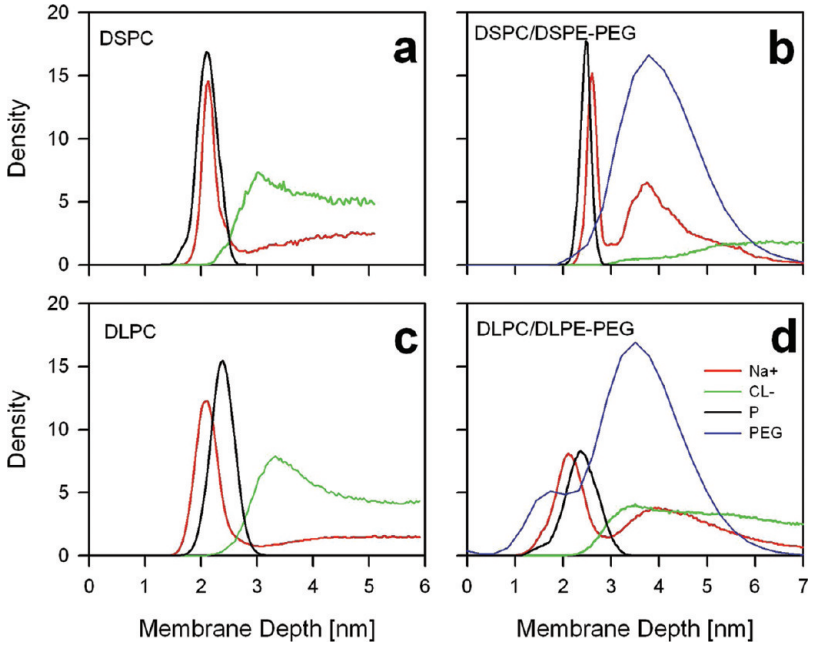

Figure 4. Mass density profiles along the bilayer normal, with the results for both leaflets averaged together: Na^+ (red line), Cl^- (green line), phosphate atoms (black line), and PEG (blue line) in (a) DSPC, (b) DSPC/DSPE-PEG, (c) DLPC, and (d) DLPC/DLPE-PEG bilayers. PEG densities were scaled 10-fold to be shown on the same scale. Zero corresponds to the bilayer center.

dx.doi.org/10.1021/la200003n |*Langmuir* 2011, 27, 7788–7798

Table 2. Percent of Na^+ Ions That Are Unbonded, Bonded with Lipids, and Bonded with PEG[a]

bilayer type	gel	liquid crystal	gel-PEG	liquid crystal-PEG
free ions	61	31	16	16
membrane-bonded ions	39	69	20	30
PEG-bonded ions			62	53

[a] The numbers are percentages. A statistically insignificant number of Na^+ ions are bound to both PEG and lipids, thus the totals do not add up to 100%.

Interactions between the Ions and the PEG Chains and Effect of PEGylation on the Ion−Headgroup Interactions. We calculated the radial distribution functions (RDF) of Na^+ ions relative to the oxygen atoms of PEG and Cl^- ions relative to the carbon atoms of PEG. As shown in Figure 5, there exists a sharp peak for the Na^+−PEG oxygen RDF that is absent for the Cl^-−PEG carbon RDF. The strength of the Na^+ oxygen peak indicates that there is a set of Na^+ ions that are effectively bound electrostatically to the PEG oxygens and that there exists no such close interaction between Cl^- ions and the PEG carbons. This can be visually seen in the snapshot of the four bilayers (Figure 3).

The binding of Na^+ ions to electronegative atoms in the lipid headgroups is not a new phenomenon. Na^+ ions are known to bind at the level of carbonyl and phosphate groups, and Cl^- ions are loosely associated with the choline group.[89,90] The number of Na^+ ions effectively bound to the carbonyl, phosphate, and PEG oxygens is listed in Table 2. As a cutoff criterion for bonding, we used the distance of 0.325 nm, corresponding to the position of the first minimum in the relevant radial distribution function, as discussed in our previous work.[64] We see that the number of bound ions is the same for both the liquid-crystalline and gel states of the PEGylated membrane whereas our previously published work on the pure system[64] indicated a greater number of bound ions in the liquid-crystalline state than in the gel state. In the PEGylated system, the greater number of Na^+ ions bound to the lipid headgroups in the liquid-crystalline state is counterbalanced by a decrease in the number of Na^+ ions bound to the PEGs. A note of caution is in order regarding the results for ion binding to lipid headgroups. The evidence that this phenomenon occurs is strong; however, there is significant quantitative disagreement regarding the strength of this binding from competing atomic potential sets.[91]

In Figure 4, the mass density profile of PEG, the Na^+ and Cl^- ions, and phosphate atoms along the membrane normal is shown for DSPC/DSPE-PEG_{2000}, DLPC/DLPE-PEG_{2000}, and the two pure systems from our previously published work.[64] The presence of PEG strongly affects the behavior of the ions. In the pure system, for both gel and liquid-crystalline membranes, the Na^+ ions strongly interact with the lipid headgroups, as indicated by the sharp peak in the density profile, and the Cl^- ions form a more diffuse cloud above the membrane headgroups because of ionic attraction to the Na^+ ions located at the headgroups. When the membrane is PEGylated, we see the emergence of a secondary peak in the Na^+ density profile, colocalized with the main peak in the PEG density profile. Because we know from our radial distribution function results that the Na^+ ions strongly interact with the PEG oxygen atoms, this is an expected result. What is interesting is how the density profile of the Cl^- ions differs between the gel and liquid-crystalline PEGylated membranes. For the liquid-crystalline membranes, the Cl^- ions have a weak peak roughly colocalized with Na^+ and PEG resulting from the ionic attraction to the Na^+ ions. This peak is absent in the gel phase. For the gel phase, PEG is completely expelled from the membrane interior (discussed in previous section) and the area per lipid is considerably smaller for the gel phase than for the liquid-crystalline phase. This will result in the PEG layer being more tightly packed, decreasing the size of water pockets in the PEG layer. Because the coordination number for Cl^- ions is ~10,[72] a reduction in the size of the water pockets in the PEG layer will thus preclude ideal bonding conditions for the Cl^- ions and make the PEG layer a less favorable environment for them.

Now that we have established that the Na^+ ions are interacting strongly with the oxygen atoms of PEG and PC, let us further examine the nature of this interaction and its effect on the PEG structure. Using the same cutoff criterion as above, we examined the number of PEG oxygen atoms that each Na^+ ion is, on average, simultaneously bound to. We found that for the DSPC/DSPE-PEG_{2000} (gel) system the total average number of oxygen atoms interacting with each Na^+ was 3.9 ± 0.1. We noticed that some Na^+ ions were forming effective cross-links between the PEG chains. For the DLPC/DLPE-PEG_{2000} (liquid-crystalline) system, our result had not quite reached an equilibrium value at the end of the simulation but appeared to be converging to the same value of approximately 3.9. However, we did not observe the same cross-linking behavior in the Na^+ ions. Because this quantity has not reached an equilibrium value, it cannot be stated with certainty that this is a real effect. This is, however, not an unexpected result; both the area per lipid of the liquid-crystalline membrane is larger and PEG is able to penetrate the membrane, thus the PEG layer will be less tightly packed in the liquid-crystalline membrane and as a result there will be less contact between different PEG polymers. The number of oxygen atoms interacting with each Na^+ ion is close to the coordination number of Na^+ (~ 4),[72] thus the Na^+ ions bound to the PEG chains are under close-to-ideal bonding conditions.

The fact that each Na^+ ion is interacting simultaneously with several oxygen atoms on the same PEG molecule indicates that the PEG polymers are in some way wrapping around the Na^+ ions. A careful examination of the trajectory using VMD showed visual evidence of this happening, as shown in Figure 6, where we can clearly see the PEG polymers forming loops around the Na^+ ions. These results are in agreement with the results found in the literature concerning PEG−cation systems[44−59] (as discussed in the Introduction).

EXPERIMENTAL RESULTS

Pressure−Area Isotherms. Figure 7 shows the pressure−area isotherms as a function of NaCl concentration for pure DSPC and DOPC and for the PC/PE-PEG_{2000} mixtures in a 9:1 molar ratio. It can be seen that for both the pure and mixed systems the level of salt concentration has a measurable effect on the results; however, the effect is different for each of the four systems.

For both the pure DSPC and DOPC systems, only the condensed phase is observed. DSPC forms an ordered crystalline monolayer, and DOPC forms a more diffuse liquid-expanded monolayer. A detailed discussion of the pure lipid system results and the effect of the salt concentration is found in the Supporting Information.

For the DSPC/DSPE-PEG_{2000} and DOPC/DOPE-PEG_{2000} mixtures, we observed starting pressures of approximately 3 and 1.5 mN/m, respectively. The system is already in a liquid phase where the pressure is finite but the surface layer is highly compressible. For both systems, the

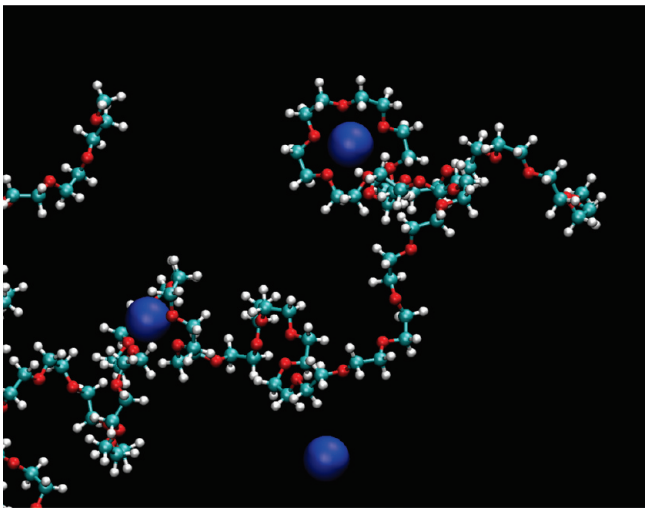

Figure 6. Visualization of the PEG polymer with the Na^+ ion demonstrating how the PEG polymers form loops around the Na^+ ions, holding them within the PEG layer. Standard atom colors are used.

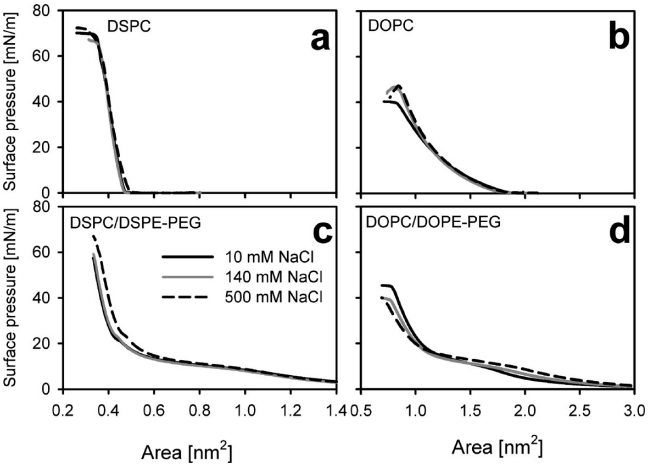

Figure 7. Pressure−area isotherms as a function of salt concentration obtained from the Langmuir film experiment for (a) DSPC and (b) DOPC and for a 9:1 molar ratio of (c) DSPC/DSPE-PEG and (d) DOPC/DOPE-PEG films.

qualitative nature of the isotherms is unchanged by altering the salt concentration; at the start of the isotherm (high area per lipid, low pressure), the pressure slowly rises as the area per lipid is decreased. The pressure then levels off to a plateau at a pressure of ~8 mN/m before rising steeply, starting at an area per lipid of ~0.6 nm^2 for DSPC/DSPE-PEG_{2000} and ~1.1 nm^2 for DOPC/DOPE-PEG_{2000} before the collapse of the film. This result can be interpreted as follows: the presence of the liquid phase results from the PEGylated lipids spreading to form a thin 2D layer that covers the surface even at the start of the isotherm. At first, the PEG layer is compressed with decreasing area per lipid, leading to a small rise in pressure. The pressure reaching a plateau corresponds to the PEG chains starting to desorb from the air−water interface into the aqueous subphase. The steep rise in pressure results from the system entering the condensed phase as the PEG chains are expelled from the surface and the monolayer takes on the crystal phase for the case of DSPC and the liquid-expanded phase for the case of DOPC. These characteristics are in good agreement with those observed previously in various PC/PE-PEG_{2000} systems.[69,70] For the DSPC/DSPE-PEG_{2000} film, an additional transition is observed at 23 mN/m. This transition is observed only when the molar concentration of DSPE-PEG_{2000} is equal to or greater than 10 mol %[68] and is generally attributed to acyl chain condensation (i.e., a conformational change in the PEG chains).[92]

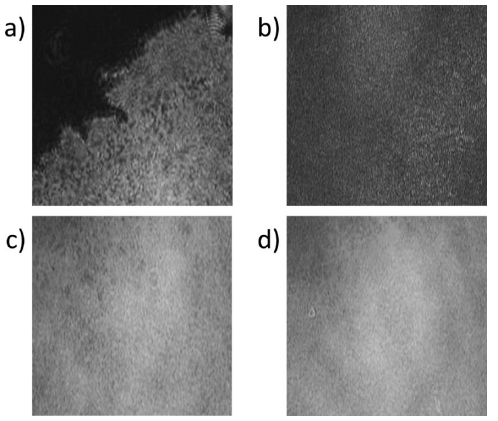

Figure 8. Brewster angle microscopy images of (a) DSPC at 0 mN/m and a mean molecular area of 0.53 nm^2, (b) a 9:1 molar ratio of DSPC/DSPE-PEG at 3 mN/m and a mean molecular area of 1.44 nm^2 (white level enhanced by a factor of 100), (c) DSPC at 41 mN/m and a mean molecular area of 0.4 nm^2, and (d) a 9:1 molar ratio of DSPC/DSPE-PEG at 40 mN/m and a mean molecular area of 0.4 nm^2. The sizes of the images are 400 and 600 μm^2.

For the DSPC/DSPE-PEG_{2000} system, the effect of the salt concentration at 140 mM is negligible. At 500 mM, however, the transition to the condensed phase takes place at a higher area per lipid. An increase in the limiting mean molecular area, determined by extrapolating the linear part of the isotherm in the condensed phase to zero pressure, from 0.46 ± 0.02 to 0.50 ± 0.02 nm^2, is observed. In the pure DSPC system, the effect at 500 mM NaCl is observed only at the beginning of the pressure increase whereas for the DSPC/DSPE-PEG_{2000} system the area per lipid is increased over the entire range of the condensed phase.

For the DOPC/DOPE-PEG_{2000} system, the effect of the salt concentration is more complex. Both of these effects, the shift of the transition point at ~8 mN/m to a higher area per lipid and the decrease in the collapse point, could be explained by PEG occupying more space at the surface with increasing salt concentration. The limiting mean molecular area increases with increasing salt concentration from 1.20 ± 0.02 nm^2 for 10 mM NaCl to 1.28 ± 0.02 nm^2 for 500 mM NaCl. This increase is accompanied by a decrease in the steepness of the pressure increase with decreasing area per lipid in the condensed-phase region (i.e., an increase in the compressibility of the film). Also, the collapse pressure decreases from 45 mN/m for 10 mM NaCl to 38 mN/m for 500 mM salt concentration. It should be noted that unlike the case of the DSPC/DSPE-PEG_{2000} system the effect of salt concentration can already be clearly seen at the physiological level (140 mM NaCl), not only at 500 mM NaCl. The increased compressibility of the film combined with the lowering of the collapse pressure with increasing salt concentration indicates that the condensed phase of the DOPC/DOPE-PEG_{2000} film is made both less stable and less ordered by the increase in the salt concentration. The shift of the transition point at ~8 mN/m to a higher area per lipid for the DOPC/DOPE-PEG_{2000} film indicates that the space occupied by PEG at the surface increases with increasing salt concentration.

BAM Images. The BAM images of the DSPC-based monolayer films are shown in Figure 8. For pure DSPC films, the molecules have already formed large domains before the start of the compression. These domains start to fuse together during the first increase in pressure, and a uniform monolayer is formed before the pressure reaches 10 mN/m.

dx.doi.org/10.1021/la200003n |*Langmuir* 2011, 27, 7788–7798

For DSPC/DSPE-PEG$_{2000}$ films at low pressures, the images were very dark; however, it is possible to observe a uniform film on the surface. The darkness of the images indicates that the film is either very thin and/or the density of the molecules is very low. At high pressure, the monolayer becomes easily visible for the DSPC/DSPE-PEG$_{2000}$ system. At all pressures, the film was observed to cover the whole area. A similar analysis was not possible for DOPC and DOPC/DOPE-PEG$_{2000}$ films; at all pressures, the images were too dark for any features to be discernible.

The BAM results for the pure system are in agreement with what is known about DSPC and DOPC: both DSPC and DOPC exhibit condensed phases at high pressure; however, DSPC forms an ordered crystalline monolayer at the surface whereas DOPC will form only the more diffuse liquid-expanded phase. This is indicated by the clearly visible domains of the crystalline phase for DSPC. In the mixed systems, we also see a clear monolayer for the DSPC/DSPE-PEG$_{2000}$ system. This result can be interpreted as indicating that the crystalline monolayer is able to form for the mixed as well as the pure system. Langmuir films of a DSPC/DSPE-PEG$_{2000}$ mixed-lipid system on a phosphate-buffered saline subphase have been studied previously by Tanwir et al.[67] using epifluorescence microscopy. They observed some immiscibility in a DSPC/DSPE-PEG$_{2000}$ film at low pressure, but the condensed phase of the system was found to be homogeneous and our results are in agreement with theirs concerning the condensed phase.

DISCUSSION

In this study, we performed 200 ns MD simulations of two PEGylated membranes at a salt concentration set to that found in blood plasma, one in the gel state and the other in the liquid-crystalline state. Our simulations were performed in combination with a Langmuir monolayer film experiment probing the effect of ion concentration on the surface of a PEGylated liposome. Our combined results indicate that the currently accepted picture[35−39,61] that the PEG surface layer can be treated as a generic hydrophilic polymer layer completely outside the membrane is inadequate.

A portion of the PEG polymer layer penetrates the membrane in the liquid-crystalline phase but not the gel phase. The looser structure of the liquid-crystalline phase allows for the entry of the PEG polymer, but the both denser and more ordered structure of the gel membrane excludes it. That PEG is found in the lipid layer should not be surprising because PEG is not a purely hydrophilic molecule. PEG is soluble in several nonpolar as well as polar solvents.[60] Our computational results indicate that PEGylation increases the area per lipid molecule and lowers the ordering in the liquid-crystalline phase while not affecting the ordering of the gel phase. The differences in the penetration of the PEG polymers into these membranes explain this effect.

As expected, PEG shows high affinity for the Na^+ cations but not for the Cl^- anions. A visual inspection of the PEG layer in our simulations (Figure 6) indicates that the PEG chains form loops around the Na^+ ions, forming electrostatic binding interactions with several oxygen atoms on the PEG chain. This behavior is well known for the PEG polymer in the presence of cations.[44−59] From the mass density profiles (Figure 4), it can be seen that the Cl^- ions colocate with the PEG layer for the case of the liquid-crystalline membrane. As a result, the PEG layer is effectively neutral, but for the case of the gel membrane, they are expelled from the PEG layer and the Na^+ cations and Cl^- anions form an effective charge double layer. As described above, the liquid-crystalline membrane shows both a larger area per lipid and some of the PEG polymer has entered the membrane. This results in the PEG layer being less dense, thus allowing room for large enough water pockets for the Cl^- ions to be hydrated between the PEG polymers in the layer. We have included movies of both rotating still images of the simulated membranes and trajectories for the membranes that demonstrate this in the Supporting Information. A schematic of the structure of the PEG layer for both the liquid-crystalline and gel membranes is shown in Figure 9.

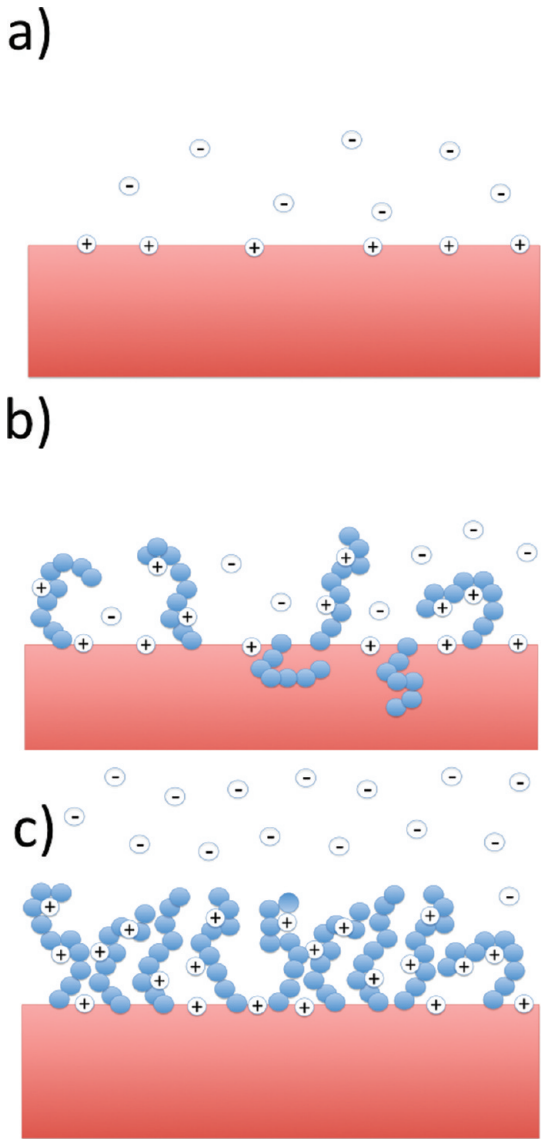

Figure 9. Diagram showing the interaction between the salt ions and the membrane for (a) the pure membrane, (b) the PEGylated liquid-crystalline membrane, and (c) the PEGylated gel membrane. The mechanism whereby the Cl^- ions are expelled from the PEG region for the case of the gel membrane is demonstrated.

For the DSPC/DSPE-PEG$_{2000}$ Langmuir film, there was an increase in the area per lipid at the highest salt concentrations, only in the condensed phase where the area per lipid is small. It is possible that the Na^+ ions binding to the PEG chains, as observed in the simulation, can cause repulsion and lead to a larger area per molecule in the condensed phase. An interesting difference between the pure and mixed DSPC-based systems is that for the pure system the increase in the area per lipid is observed only at low surface pressures of <20 mN/m. This could be explained as

the effect in the pure system resulting from Na^+ ions binding to the phosphate groups, as we have seen in our previous work,[64] and this effect being overcome at higher pressures whereas the equivalent effect relating to PEG chains is not.

The results of this study also may have pharmaceutical significance. After their administration, liposomes bind proteins in the bloodstream and tissues, leading to their recognition by macrophages and subsequent removal and degradation.[3] PEGylation decreases the protein binding, but the precise mechanisms are not fully understood.[93−100] In general, the surface charge of the liposome is known to enhance opsonization and increase the rate of elimination.[3]

A neutral polymer layer should act as a neutral screening layer and reduce the interactions with proteins. Our liquid-crystalline system showed a neutral PEG layer, but for our gel system, we observed an effectively charged PEG layer at the physiological salt concentration. It is possible that a lower fraction of PEGylated lipid will also result in an effectively neutral PEG coating. This might explain the conflicting experimental results for the effect of PEGylation on liposome−protein interactions.[93−100] It is important to note that intravenously applied liposomes are usually in the gel state. In this case, at our PEG density the liposomes are not neutral and the salt interactions may increase the elimination rate of liposomes from the bloodstream. Taken together, our findings indicate that the overall behavior of the PEGylated liposome surface is more complex than previously thought and ions in the blood plasma may interfere with the properties of the PEG layer and subsequently influence the liposome−protein interactions. These aspects should be taken into account when nanoparticle coatings are designed.

It should also be noted that Na^+ and Cl^- are not the only ions found in blood plasma and other ions may also interact with the PEGylated membrane in a similar fashion. In particular, divalent ions such as Ca^{2+} are expected to have an even stronger effect on the PEG layer.

The penetration of PEG into the liquid-crystalline lipid bilayer is an interesting observation. Such an interaction may affect the structure and permeability of the lipid membrane and might lead, for example, to premature drug leakage from the liposomes. This may also affect the liposomes that are originally in the gel state but undergo a shift to the liquid-crystalline state. The mechanism normally involves the formation of defect structures that results in a peak in the membrane permeability that can be used for triggered release,[24] and clearly the insertion of PEG chains into the lipid bilayer may affect this process. There are experimental reports that show that PEG induces an increase in liposome permeability.[101,102] In the gel state, the PEG did not dip into the bilayer, and in that case, we did not expect any PEG-induced changes in liposomal drug release.

■ ASSOCIATED CONTENT

Supporting Information. The validation of our all-atom model for the PEG polymer. Verification that our system is not affected by finite size effects. Effect of PEGylation on the water ordering in the vicinity of the membrane. Animation of DSPC and DLPC. A detailed discussion of the pure lipid system results and the effect of the salt concentration. Simulations of PEG in water solution. Graph of the deuterium order parameter. Pressure−area isotherms for the pure systems. This material is available free of charge via the Internet at http://pubs.acs.org.

■ AUTHOR INFORMATION

Corresponding Author
*E-mail: alex.bunker2@gmail.com.

■ ACKNOWLEDGMENT

This work was supported by the Natural Sciences and Engineering Research Council of Canada (M.K.), the Academy of Finland (T.R.), and the Emil Altonen Foundation (A.B.). Computational resources have been provided by SharcNet and the Finnish IT Centre for Science.

■ REFERENCES

(1) Farokhzad, O. C.; Langer, R. Impact of nanotechnology on drug delivery. *ACS Nano* **2009**, *3*, 16–20.

(2) Lasic, D. D. Novel applications of liposomes. *Trends Biotechnol.* **1998**, *16*, 307–321.

(3) Yan, X.; Scherphof, G. L.; Kamps, J. A. A. M. Liposome opsonization. *J. Liposome Res.* **2005**, *15*, 109–139.

(4) Moghimi, S. M.; Szebeni, J. Stealth liposomes and long circulating nanoparticles: critical issues in pharmacokinetics, opsonization and protein-binding properties. *Prog. Lipid Res.* **2003**, *42*, 463–478.

(5) Romberg, B.; Oussoren, C.; Snel, C. J.; Carstens, M. G.; Hennink, W. E.; Storm, G. Pharmacokinetics of poly(hydroxyethyl-l-asparagine)-coated liposomes is superior over that of PEG-coated liposomes at low lipid dose and upon repeated administration. *Biochim. Biophys. Acta, Biomembr.* **2007**, *1768*, 737–743.

(6) Klibanov, A. L.; Maruyama, K.; Torchilin, V. P.; Huang, L. Amphipathic polyethyleneglycols effectively prolong the circulation time of liposomes. *FEBS Lett.* **1990**, *268*, 235–237.

(7) Allen, T. M. Long-circulating (sterically stabilized) liposomes for targeted drug delivery. *Trends Pharmacol. Sci.* **1994**, *15*, 215–220.

(8) Torchilin, V. P. Recent advances with liposomes as pharmaceutical carriers. *Nat. Rev. Drug Discovery* **2005**, *4*, 145–160.

(9) Gabizon, A. A.; Shmeeda, H.; Zalipsky, S. Pros and cons of the liposome platform in cancer drug targeting. *J. Liposome Res.* **2006**, *16*, 175–183.

(10) Cattel, L.; Ceruti, M.; Dosio, F. From conventional to stealth liposomes: a new frontier in cancer chemotherapy. *Tumori* **2003**, *89*, 237–249.

(11) Sapra, P.; Tyagi, P.; Allen, T. M. Ligand-targeted liposomes for cancer treatment. *Curr. Drug Delivery* **2005**, *2*, 369–381.

(12) Gabizon, A. A. Pegylated liposomal doxorubicin: metamorphosis of an old drug into a new form of chemotherapy. *Cancer Invest.* **2001**, *19*, 424–436.

(13) Gabizon, A. A.; Tzemach, D.; Mak, L.; Bronstein, M.; Horowitz, A. T. Dose dependency of pharmacokinetics and therapeutic efficacy of pegylated liposomal doxorubicin (DOXIL) in murine models. *J. Drug Targeting* **2002**, *10*, 539–548.

(14) Bakker-Woudenberg, I. A. J. M. Long-circulating sterically stabilized liposomes as carriers of agents for treatment of infection or for imaging infectious foci. *Int. J. Antimicrob. Agents* **2002**, *19*, 299–311.

(15) Felgner, P. L.; Ringold, G. M. Cationic liposome-mediated transfection. *Nature* **1989**, *337*, 387–388.

(16) Torchilin, V. P. Liposomes as delivery agents for medical imaging. *Mol. Med. Today* **1996**, *2*, 242–249.

(17) Olivier, J.-C. Drug transport to brain with targeted nanoparticles. *NeuroRx* **2005**, *2*, 108–119.

(18) Pasut, G.; Veronese, F. M. PEGylation for improving the effectiveness of therapeutic biomolecules. *Drugs Today* **2009**, *45*, 687–695.

(19) Nawalany, K.; Kozik, B.; Kepczynski, M.; Zapotoczny, S.; Kumorek, M.; Nowakowska, M.; Jachimska, B. Properties of polyethylene glycol supported tetraaryporphyrin in aqueous solution and its interaction with liposomal membranes. *J. Phys. Chem. B* **2008**, *112*, 12231–12239.

(20) Moghimi, S. M.; Hunter, A. C.; Murray, J. C. Long-circulating and target-specific nanoparticles: theory to practice. *Pharmacol. Rev.* **2001**, *53*, 283–318.
(21) Vonarbourg, A.; Passirani, C.; Saulnier, P.; Benoit, J.-P. Parameters influencing the stealthiness of colloidal drug delivery systems. *Biomaterials* **2006**, *27*, 4356–4373.
(22) Woodle, M. C.; Newman, M. S.; Cohen, J. A. Sterically stabilized liposomes: physical and biological properties. *J. Drug Targeting* **1994**, *2*, 397–403.
(23) Woodle, M. C. Controlling liposome blood clearance by surface-grafted polymers. *Adv. Drug. Delivery Rev.* **1998**, *32*, 139–152.
(24) Paasonen, L.; Romberg, B.; Storm, G.; Yliperttula, M.; Urtti, A.; Hennink, W. E. Temperature-sensitive poly(*N*-(2-hydroxypropyl)methacrylamide mono/dilactate)-coated liposomes for triggered contents release. *Bioconjugate Chem.* **2007**, *18*, 2131–2136.
(25) Hristova, K.; Needham, D. The influence of polymer-grafted lipids on the physical properties of lipid bilayers: a theoretical study. *J. Colloid Interface Sci.* **1994**, *168*, 302–314.
(26) Rex, S.; Zuckermann, M. J.; Lafleur, M.; Silvius, J. R. Experimental and Monte Carlo simulation studies of the thermodynamics of polyethyleneglycol chains grafted to lipid bilayers. *Biophys. J.* **1998**, *75*, 2900–2914.
(27) Thakkar, F. M.; Ayappa, K. G. Effect of polymer grafting on the bilayer gel to liquid-crystalline transition. *J. Phys. Chem. B* **2010**, *114*, 2738–2748.
(28) Baulin, V. A.; Zhulia, E. B.; Halperin, A. Self-consistent field theory of brushes of neutral water-soluble polymers. *J. Chem. Phys.* **2003**, *119*, 10977–10987.
(29) Alexander, S. Adsorption of chain molecules with a polar head. A scaling description. *J. Phys. (Paris)* **1977**, *38*, 983–987.
(30) de Gennes, P. G. Conformations of polymers attached to an interface. *Macromolecules* **1980**, *13*, 1069–1075.
(31) Goujon, F.; Malfreyt, P.; Tildesley, D. J. Mesoscopic simulation of entanglements using dissipative particle dynamics: Application to polymer brushes. *J. Chem. Phys.* **2008**, *129*, 034902.
(32) Grest, G. S. Grafted polymer brushes: a constant surface pressure molecular dynamics simulation. *Macromolecules* **1994**, *27*, 418–426.
(33) Laradji, M.; Guo, H.; Zuckermann, M. Off-lattice Monte Carlo simulation of polymer brushes in good solvents. *Phys. Rev. E* **1994**, *49*, 3199–3206.
(34) Pal, S.; Seidel, C. Dissipative particle dynamics simulations of polymer brushes: comparison with molecular dynamics simulations. *Macromol. Theory Simul.* **2006**, *15*, 668–673.
(35) Kenworthy, A. K.; Simon, S. A.; McIntosh, T. J. Structure and phase behavior of lipid suspensions containing phospholipids with covalently attached poly(ethylene glycol). *Biophys. J.* **1995**, *68*, 1903–1920.
(36) Kuhl, T. L.; Leckband, D. E.; Lasic, D. D.; Israelachvili, J. N. Modulation of interaction forces between bilayers exposing short-chained ethylene oxide headgroups. *Biophys. J.* **1994**, *66*, 1479–1488.
(37) Pantusa, M.; Bartucci, R.; marsh, D.; Sportelli, L. Shifts in chain-melting transition temperature of liposomal membranes by polymer-grafted lipids. *Biochim. Biophys. Acta* **2003**, *1614*, 165–170.
(38) Warriner, H. E.; Keller, S. L.; Idziak, S. H. J.; Slack, N. L.; Davidson, P.; Zasadzinski, J. A.; Safinya, C. R. The influence of polymer molecular weight in lamellar gels based on PEG-lipids. *Biophys. J.* **1998**, *75*, 272–293.
(39) Needham, D.; Kim, D. H. PEG-covered lipid surfaces: bilayers and monolayers. *Colloids Surf., B* **2000**, *18*, 183–195.
(40) Cohen, J. A.; Khorosheva, V. A. Electrokinetic measurement of hydrodynamic properties of grafted polymer layers on liposome surfaces. *Colloids Surf., A* **2001**, *195*, 113–127.
(41) Janzen, J.; Song, X.; Brooks, D. E. Interfacial thickness of liposomes containing poly(ethylene glycol)-cholesterol from electrophoresis. *Biophys. J.* **1996**, *70*, 313–320.
(42) Müller-Plathe, F.; van Gunsteren, W. F. Computer simulation of a polymer electrolyte: lithium iodide in amorphous poly(ethylene oxide). *J. Chem. Phys.* **1995**, *103*, 4745–4756.
(43) Laasonen, K.; Klein, M. L. Molecular dynamics simulations of the structure and ion diffusion in poly(ethylene oxide). *J. Chem. Soc., Faraday Trans* **1995**, *91*, 2633–2638.
(44) Borodin, O.; Smith, G. D. Molecular dynamics simulations of poly(ethylene oxide)/LiI melts. 1. Structural and conformational properties. *Macromolecules* **1998**, *31*, 8396–8406.
(45) Neyertz, S.; Brown, D. Phase separation upon heating in model PEO_x NaI polymer electrolytes. *Electrochim. Acta* **1998**, *43*, 1343–1347.
(46) Siqueira, L. J. A.; Ribeiro, M. C. C. Molecular dynamics simulation of the polymer electrolyte poly(ethylene oxide)/$LiClO_4$. I. Structural properties. *J. Chem. Phys.* **2005**, *122*, 194911.
(47) van Zon, A.; Mos, B.; Verkerk, P.; de Leeuw, S. W. On the dynamics of PEO-NaI polymer electrolytes. *Electrochim. Acta* **2001**, *46*, 1717–1721.
(48) Annis, B. K.; Kim, M.-H.; Wignall, G. D.; Borodin, O.; Smith, G. D. A study of the influence of LiI on the chain conformations of poly(ethylene oxide) in the melt by small-angle neutron scattering and molecular dynamics simulations. *Macromolecules* **2000**, *33*, 7544–7548.
(49) Diddens, D.; Heuer, A.; Borodin, O. Understanding the lithium transport within a Rouse-based model for a PEO/LiTFSI polymer electrolyte. *Macromolecules* **2010**, *43*, 2028–2036.
(50) Duan, Y.; Halley, J. W.; Curtiss, L.; Redfern, P. Mechanisms of lithium transport in amorphous polyethylene oxide. *J. Chem. Phys.* **2005**, *122*, 054702.
(51) Annis, B. K.; Badyal, Y. S.; Simonson, J. M. Neutron-scattering determination of the Li^+ environment in an aqueous poly(ethylene oxide) solution. *J. Phys. Chem. B* **2004**, *108*, 2554–2556.
(52) Bogan, M. J.; Agnes, G. R. Poly(ethylene glycol) doubly and singly cationized by different alkali metal ions: relative cation affinities and cation-dependent resolution in a quadrupole ion trap mass spectrometer. *J. Am. Soc. Mass. Spectrom.* **2002**, *13*, 177–186.
(53) Habenschuss, A. Structure of an aqueous poly(ethylene oxide) LiI solution from X-ray scattering. *J. Mol. Liq.* **2007**, *136*, 79–82.
(54) Hakem, I. F.; Lal, J.; Bockstaller, M. R. Binding of monovalent ions to PEO in solution: relevant parameters and structural transitions. *Macromolecules* **2004**, *37*, 8431–8440.
(55) Hakem, I. F.; Lal, J.; Bockstaller, M. R. Mixed solvent effect on lithium-coordination to poly(ethylene oxide). *J. Polym. Sci., Part B: Polym. Phys.* **2006**, *44*, 3642–3650.
(56) Hortal, A. R.; Hurtado, P.; Martinez-Haya, B.; Arregul, A.; Bañares, L. Poly(ethylene glycol) cationization with alkali metals in matrix-assisted laser desorption ionization investigated with the solvent-free method. *Appl. Phys. A: Mater. Sci. Process.* **2008**, *92*, 859–863.
(57) Rhodes, C. P.; Khan, M.; French, R. Crystalline phases of poly(ethylene oxide) oligomers and sodium triflate: changes in coordination and conformation with chain length. *J. Phys. Chem. B* **2002**, *106*, 10330–10337.
(58) Stolwijk, N. A.; Wiencierz, M.; Obeidi, S. Mass and charge transport in the PEO-NaI polymer electrolyte system: effects of temperature and salt concentration. *Faraday Discuss.* **2007**, *134*, 157–169.
(59) Triolo, A.; Celso, F. L.; Arrighi, V.; Strunz, P.; Lechner, R. E.; Mastragostino, M.; Passerini, S.; Annis, B. K.; Triolo, R. Structural and dynamical characterization of melt PEO-salt mixtures. *Physica A* **2002**, *304*, 308–313.
(60) Dinç, C. Ö.; Kibarer, G.; Güner, A. Solubility profiles of poly(ethylene glycol)/solvent systems. II. Comparison of thermodynamic parameters from viscosity measurements. *J. Appl. Polym. Sci.* **2010**, *117*, 1100–1119.
(61) Hill, R. J. Hydrodynamics and electrokinetics of spherical liposomes with coatings of terminally anchored poly(ethylene glycol): numerically exact electrokinetics with self-consistent mean-field polymer. *Phys. Rev. E* **2004**, *70*, 051406.
(62) Nowakowska, M.; Nawalany, K.; Kepczyński, M.; Krawczyk, Z. Novel nanostructural hybride materials for photodynamic theraphy. *Macromol. Symp.* **2008**, *279*, 132–137.
(63) Koynova, R.; Caffrey, M. Phases and phase transitions of the phosphatidylcholines. *Biochim. Biophys. Acta, Biomembr.* **1998**, *1376*, 91–145.

(64) Stepniewski, M.; Bunker, A.; Pasenkiewicz-Gierula, M.; Karttunen, M.; Róg, T. Effects of the lipid bilayer phase state on the water membrane interface. *J. Phys. Chem. B* **2010**, *114*, 11784–11792.

(65) Marković, D. UV-induced reaction kinetics in dilinoleoylphosphatidylcholine monolayers with incorporated photosensitizers. *J. Serb. Chem. Soc.* **2006**, *71*, 349–356.

(66) FengKui, M.; Jing, W.; Uematsu, S.; Akahori, Y. Study on monolayer of vitamin E and phosphatidylcholines. *Acta Phys.-Chim. Sin.* **1995**, *11*, 1077–1083.

(67) Tanwir, K.; Tsoukanova, V. Lateral distribution of a poly-(ethylene glycol)-grafted phospholipid in phosphocholine monolayers studied by epifluorescence microscopy. *Langmuir* **2008**, *24*, 14078–14087.

(68) Xu, Z.; Holland, N. B.; Marchan, R. E. Conformations of short-chain poly(ethylene oxide) lipopolymers at the air−water interface: a combined film balance and surface tension study. *Langmuir* **2001**, *17*, 377–383.

(69) Lozano, M. M.; Longo, M. L. Complex formation and other phase transformations mapped in saturated phosphatidylcholine/DSPE-PEG2000 monolayers. *Soft Matter* **2009**, *5*, 1822–1834.

(70) Chou, T.-H.; Chu, I.-M. Thermodynamic characteristics of DSPC/DSPE-PEG2000 mixed monolayers on the water subphase at different temperatures. *Colloids Surf., B* **2003**, *27*, 333–344.

(71) Jorgensen, W. L.; Tirado-Rives, J. The OPLS potential functions for proteins. Energy minimizations for crystals of cyclic peptides and crambin. *J. Am. Chem. Soc.* **1988**, *110*, 1657–1666.

(72) Patra, M.; Karttunen, M. Systematic comparison of force fields for microscopic simulations of NaCl in aqueous solutions: diffusion, free energy of hydration, and structural properties. *J. Comput. Chem.* **2004**, *25*, 678–689.

(73) Róg, T.; Vattulainen, I.; Karttunen, M. Modelling glycolipids: take one. *Cell. Mol. Biol. Lett.* **2005**, *10*, 625–630.

(74) Róg, T.; Vattulainen, I.; Bunker, A.; Karttunen, M. Glycolipid membranes through atomistic simulations: effects of glucose and galactose head groups on lipid bilayer properties. *J. Phys. Chem. B* **2007**, *111*, 10146–10154.

(75) Róg, T.; Martinez-Seara, H.; Munck, N.; Orešič, M.; Karttunen, M.; Vattulainen, I. Role of cardiolipins in the inner mitochondrial membrane: insight gained through atom-scale simulations. *J. Phys. Chem. B* **2009**, *113*, 3413–3422.

(76) Takaoka, Y.; Pasenkiewicz-Gierula, M.; Miyagawa, H.; Kitamura, K.; Tamura, Y.; Kusumi, A. Molecular dynamics generation of nonarbitrary membrane models reveals lipid orientational correlations. *Biophys. J.* **2000**, *79*, 3118–3138.

(77) Wong-ekkabut, J.; Miettinen, M. S.; Dias, C.; Karttunen, M. Static charges cannot drive a continuous flow of water molecules through a carbon nanotube. *Nat. Nanotechnol.* **2010**, *5*, 555–557.

(78) Jorgensen, W. L.; Chandrasekhar, J.; Madura, J. D.; Impey, R. W.; Klein, M. L. Comparison of simple potential functions for simulating liquid water. *J. Chem. Phys.* **1983**, *79*, 926–935.

(79) Lindahl, E.; Hess, B.; van der Spoel, D. GROMACS 3.0: a package for molecular simulation and trajectory analysis. *J. Mol. Mod.* **2001**, *7*, 306–317.

(80) Hess, B.; Bekker, H.; Berendsen, H. J. C.; Fraaije, J. G. E. M. LINCS: a linear constraint solver for molecular simulations. *J. Comput. Chem.* **1997**, *18*, 1463–1472.

(81) Nosé, S. A unified formulation of the constant temperature molecular dynamics methods. *J. Chem. Phys.* **1984**, *81*, 511–519.

(82) Hoover, W. G. Canonical dynamics: equilibrium phase-space distributions. *Phys. Rev. A* **1985**, *31*, 1695–1697.

(83) Parrinello, M.; Rahman, A. Polymorphic transitions in single crystals: a new molecular dynamics method. *J. Appl. Phys.* **1981**, *52*, 7182–7190.

(84) Essman, U.; Perela, L.; Berkowitz, M. L.; Darden, T.; Lee, H.; Pedersen, L. G. A smooth particle mesh Ewald method. *J. Chem. Phys.* **1995**, *103*, 8577–8593.

(85) Karttunen, M.; Rottler, J.; Vattulainen, I.; Sagui, C.; Feller, S. Electrostatics in biomolecular simulations: where are we now and where are we heading. *Curr. Top. Membr.* **2008**, *60*, 49–89.

(86) Kučerka, N.; Nagle, J. F.; Sachs, J. N.; Feller, S. E.; Pencer, J.; Jackson, A.; Katsaras, J. Lipid bilayer structure determined by the simultaneous analysis of neutron and X-ray scattering data. *Biophys. J.* **2008**, *95*, 2536–2635.

(87) McConnell, H. M.; Radhakrishnan, A. Condensed complexes of cholesterol and phospholipids. *Biochim. Biophys. Acta, Biomembr.* **2003**, *1610*, 159–173.

(88) Nagle, J. F.; Tristram-Nagle, S. Structure of lipid bilayers. *Biochim. Biophys. Acta, Biomembr.* **2000**, *1469*, 159–195.

(89) Berkowitz, M. L.; Bostick, D. L.; Pandit, S. Aqueous solutions next to phospholipid membrane surfaces: insights from simulations. *Chem. Rev.* **2006**, *106*, 1527–1539.

(90) Zhao, W.; Róg, T.; Gurtovenko, A. A.; Vattulainen, I.; Karttunen, M. Atomic-scale structure and electrostatics of anionic palmitoyloleoylphosphatidylglycerol lipid bilayers with Na^+ counterions. *Biophys. J.* **2007**, *92*, 1114–1124.

(91) Miettinen, M. S.; Gurtovenko, A. A.; Vattulainen, I.; Karttunen, M. Ion dynamics in cationic lipid bilayer systems in saline solutions. *J. Phys. Chem. B* **2009**, *113*, 9226–9234.

(92) Baekmark, T. R.; Wiesenthal, T.; Kuhn, P.; Albersdörfer, A.; Nuyken, O.; Merkel, R. A systematic infrared reflection-absorption spectroscopy and film balance study of the phase behavior of lipopolymer monolayers at the air−water interface. *Langmuir* **1999**, *15*, 3616–3626.

(93) Chui, G. N. C.; Bally, M. B.; Mayer, L. D. Selective protein interactions with phosphatidylserine containing liposomes alter the steric stabilization properties of poly(ethylene glycol). *Biochim. Biophys. Acta* **2001**, *1510*, 56–69.

(94) Du, H.; Chandaroy, P.; Hui, S. W. Grafted poly-(ethylene glycol) on lipid surfaces inhibits protein adsorption and cell adhesion. *Biochim. Biophys. Acta* **1997**, *1326*, 236–248.

(95) Efremova, N. V.; Bondurant, B.; O'Brian, D. F.; Leckband, D. E. Measurements of interbilayer forces and protein adsorption on uncharged lipid bilayers displaying poly(ethylene glycol) chains. *Biochemistry* **2000**, *39*, 3441–3451.

(96) Hashizaki, K.; Taguchi, H.; Sakai, H.; Abe, M.; Saito, Y.; Ogawa, N. Carboxyflourine leakage from poly(ethylene glycol)-grafted liposomes induced by the interaction with serum. *Chem. Pharm. Bull.* **2006**, *54*, 80–84.

(97) Szebeni, J.; Baranyi, L.; Savay, S.; Milosevits, J.; Bunger, R.; Laverman, P.; Metselaar, J. M.; Storm, G.; Chanan-Khan, A.; Liebes, L.; Muggia, F. M.; Cohen, R.; Barenholz, Y.; Alving, C. R. Role of complement activation in hypersensitivity reactions to doxil and hynic PEG liposomes: experimental and clinical studies. *J. Liposome Res.* **2002**, *12*, 165–172.

(98) Xu, Z.; Marchant, R. E. Adsorption of plasma proteins on polyethylene oxide-modified lipid bilayers studied by total internal reflection flourescence. *Biomaterials* **2000**, *21*, 1075–1083.

(99) Price, M. E.; Cornelius, R. M.; Brash, J. L. Protein adsorption to polyethylene glycol modified liposomes from fibrinogen solution and from plasma. *Biochim. Biophys. Acta* **2001**, *1512*, 191–205.

(100) Semple, S. C.; Chonn, A.; Cullis, P. R. Interactions of liposomes and lipid-based carrier systems with blood proteins: Relation to clearance behavior in vivo. *Adv. Drug Delivery Rev.* **1998**, *32*, 3–17.

(101) Nikolova, A. N.; Jones, M. N. Effect of grafted PEG-2000 on the size and permeability of vesicles. *Biochim. Biophys. Acta* **1996**, *1304*, 120–128.

(102) Nicholas, A. R.; Scott, M. J.; Kennedy, N. I.; Jones, M. N. Effect of grafted polyethylene glycol (PEG) on the size, encapsulation efficiency and permeability of vesicles. *Biochim. Biophys. Acta* **2000**, *1463*, 167–178.